Potential Use of a Combined Ozone and Zeolite System for Gaseous Toluene Elimination

ARTICLE *in* JOURNAL OF HAZARDOUS MATERIALS · JUNE 2007

Impact Factor: 4.53 · DOI: 10.1016/j.jhazmat.2006.08.077 · Source: PubMed

3 AUTHORS:

Christopher Y H Chao
The Hong Kong University of Science and T…
150 PUBLICATIONS **2,606** CITATIONS
SEE PROFILE

Philip CW Kwong
University of Adelaide
27 PUBLICATIONS **279** CITATIONS
SEE PROFILE

K.S. Hui
Hanyang University
110 PUBLICATIONS **1,373** CITATIONS
SEE PROFILE

Available online at www.sciencedirect.com
ScienceDirect
Journal of Hazardous Materials 143 (2007) 118–127
Journal of Hazardous Materials
www.elsevier.com/locate/jhazmat

Potential use of a combined ozone and zeolite system for gaseous toluene elimination

C.Y.H. Chao *, C.W. Kwong, K.S. Hui

Department of Mechanical Engineering, The Hong Kong University of Science and Technology, Clear Water Bay, Kowloon, Hong Kong, China

Received 26 April 2006; received in revised form 31 August 2006; accepted 31 August 2006
Available online 16 September 2006

Abstract

This study investigated the performance of a combined ozone and zeolite system in eliminating gaseous toluene which is a major contaminant in many industrial and indoor environments. The hypothesis that the removal of toluene by ozone can be substantially affected by confining the oxidation reaction in a zeolite structure was evaluated. The degradation of toluene seemed to be contributed by the active oxygen atom generated from the decomposition of ozone at the Lewis acid sites in the zeolite 13X. Air containing toluene levels at 1.5, 2 and 3 ppm was injected with ozone in the range of 0–6 ppm before being vented into a fixed amount of 3600 g zeolite 13X with 90 mm bed-length. The experimental results showed that the elimination rate of toluene was significantly enhanced when compared to using zeolite or ozone alone. In particular, over 90% of the 1.5 ppm toluene was removed when 6 ppm ozone was used at 40% relative humidity level. Deactivation of the zeolite 13X after a few hours of reactions under the current experimental conditions was probably due to the adsorbed water, carbon dioxide and the reaction by-products. The residue species left in the zeolite and the intermediate species in the exhaust gas stream were characterized by FT-IR, GC–MS and HP-LC methods, respectively. A distinctive peak of O atom attached to the Lewis acid site at 1380 cm^{-1} was found in the FT-IR spectrum and trace amount of aldehydes was found to be the reaction by-products.

Keywords: Zeolite; Ozone; Toluene; Catalytic oxidation

1. Introduction

Concern of occupational exposure to volatile organic compounds (VOCs) has been increasing. VOCs have been associated with various health-related problems including eyes irritation, nervous system effects, liver toxicity, cancers, etc. [1–5]. Common way to reduce the harmful effect is to dilute the VOCs by ventilation. The other effective ways to control the VOCs level include adsorption, thermal or catalytic oxidation, photo-catalytic oxidation and plasma. Porous media such as activated carbon and zeolite possess large specific areas and have high adsorption capacity. They are frequently employed in traditional adsorption air purification systems to adsorb gases or odours [6–9]. Pollutant adsorption by activated carbon provides a cost-effective and feasible way to minimize the pollutant level. Granular activated carbon has been proven to be an efficient adsorbent for removing VOCs in industrial environments. Zhao et al. [9] compared the VOC adsorption performance on activated carbons and zeolites. They concluded that the hydrophobic MCM-41 was a potential adsorbent for the removal of high concentrations VOCs at high humidity environments. Hydrophobic zeolites were the potential adsorbents in removing VOCs in low concentrations with high humidity. Activated carbon adsorbents are a good choice for use in adsorption systems because they are cost-effective materials. However, these adsorption techniques only transfer the contaminants to another phase rather than eliminating them. Some researchers [10–12] use thermal or catalytic combustion to remove VOCs. These techniques can convert organic pollutants into a mixture of CO_2 and H_2O by catalytic reactions. Alvarez-Merino et al. [12] used tungsten oxide supported on activated carbon catalysts for toluene catalytic combustion. A flow of 500 ppm toluene was incinerated at 350 °C and a high removal efficiency of 87% was achieved. They found that CO, CO_2 and H_2O were the products of the incineration process. The drawbacks of the catalytic incineration are that significant amount of energy was required to sustain the

* Corresponding author. Tel.: +852 2358 7210; fax: +852 2358 1543.
E-mail address: meyhchao@ust.hk (C.Y.H. Chao).

0304-3894/$ – see front matter © 2006 Elsevier B.V. All rights reserved.
doi:10.1016/j.jhazmat.2006.08.077

incineration process and the associated disposal problems of the spent catalyst. Apart from catalytic incineration, the uses of photocatalytic reactions to decompose organic compounds were studied by numerous researchers [13–16]. Hodgson et al. [16] concluded that the ultra-violet photocatalytic oxidation (UV-PCO) device has high reaction efficiency towards the VOCs commonly found in indoor environments. However, the short lifetime of the UV lamp may increase the operation cost of UV-PCO and the intermediates produced during the PCO process can occupy the active sites of the catalyst surface and may result in deactivation of the catalyst. This is the concern with respect to the use of photo-catalytic air cleaning technology in indoor environments. Similar to the mechanisms of photo-catalytic oxidations, some researchers used plasma to generate reactive species including energetic electrons and atomic oxygen to decompose VOCs into CO_2 and H_2O [17–20]. Oh et al. [17] used various kinds of zeolites to decompose toluene in surface discharge plasma. Their results showed that the decomposition efficiency depended on the position of the zeolite and the toluene adsorption capacity. They also mentioned that the active oxygen species generated from the plasma could enhance the oxidation of the adsorbed toluene. In addition, Einaga et al. [19] investigated the benzene decomposition efficiency on a silent discharge plasma coupled with manganese oxide catalysts. They found that the benzene conversion and the CO_2 selectivity were greatly enhanced by using MnO_2 in silent discharge plasma.

In addition to the above air purification technologies, several studies evaluated the use of ozone alone to remove indoor VOCs [21–24] and discovered that the VOC removal efficiencies were very low and certain by-products were produced [21]. The high level of residual ozone may impose health problems to the occupants [25,26]. Weschler [27] stated that the reaction between the residual ozone and the unsaturated VOCs containing one or more unsaturated carbon–carbon bonds in the indoor air may also lead to the formation of intermediate species such as aldehydes and organic acids. Fine mode particles can also be generated under the complicated ozone chemistry [28,29]. Chen et al. [30] evaluated several types of air cleaners for the removal of multiple VOCs in indoor air including sorption filtration, UV-PCO and ozone oxidation. They concluded that the sorption filtration generally provided a good removal efficiency of the VOCs, while the UV-PCO could convert most indoor VOCs into CO_2 and water. However, they did not recommend the use of ozone air cleaners for the removal of VOCs due to the fact that the removal efficiencies were low and they were likely to increase the indoor ozone concentration to an unsafe level.

Despite the various problems of using ozone in air purification, it should be noted that ozone is in fact a very strong oxidizing agent. The current study aimed to explore the performance of pollutant destruction when the pollutant and various levels of ozone are confined to react in a zeolite structure. The idea comes from the fact that zeolite is a very good adsorbent for certain VOCs and if both the VOCs and ozone can be trapped inside the pores, it may be possible that the reaction can be enhanced. From this perspective, zeolite may perform the function as a catalyst in the overall contaminant degradation process to decompose ozone into atomic oxygen and to provide a confined space in order to extend the residence time for the VOC–ozone reactions. Moreover, zeolite could also be treated as an adsorbent for the by-products that are generated by the VOC–ozone reactions. These by-products may just be adsorbed or be subsequently destructed. Experiments were designed to verify if the above hypotheses are valid or not and to explore potential applications of this kind of system. Recent researches [31–33] have demonstrated the gas-phase catalytic ozonation of air pollutants on various systems. Kastner et al. [32,33] used recycled materials for the gas-phase catalytic ozonation of high volume low concentration emissions. They concluded that a high conversion efficiency of gaseous reduced sulfur compounds could be achieved at room temperature. However, the detailed studies on the effect of the inlet concentration of ozone and the pollutant to the decomposition of toluene in zeolite 13X in a large scale system have rarely been discussed in the past. Zeolite was selected for our experiments instead of activated carbon because it demonstrates a good regeneration properties and the structure is relatively stable to the exposure of ozone. Ozone can change the structure of activated carbon by enlarging pores and creating new pores [34,35]. Gasification occurs and CO_2 are produced when O_3 oxidizes the activated carbon surface. CO_2 exits the surface and creates new pores [36]. The consumption and the change of the carbon surface structure may influence the performance of VOC–ozone reaction and the regeneration of the media and hence activated carbon was not used in this study.

Zeolite 13X with pellet size 3–5 mm was used for the experiments and it has been considered as a favourable adsorbent for both water and VOCs. Zeolite 13X is a faujasite molecular sieve with 7.4 Å diameter pores and a three-dimensional pore structure [37,38]. Ozone (5.8 Å) [39] and toluene (5.85 Å) [40] are accessible to the pore of the zeolite 13X. The large surface area zeolite can potentially be utilized for the application of pollutant adsorption and subsequent catalytic reactions. The active sites can catalyze the degradation of large molecules [41] and the VOC–ozone reaction can be enhanced to have higher removal efficiencies than the system only containing zeolite or ozone alone. With the existence of zeolite as an adsorption site and potential catalyst, there seems to be a possibility to enhance the reaction rate between ozone and the VOCs, while the level of residual ozone can be minimized. Ozone level in the range of 0–6 ppm was employed in this study. The ozone level higher than 6 ppm was not tried because of the concern that significant amount of residual ozone may be generated. The zeolite–ozone system can be regenerated with minimum energy input and thus the operation cost of the air purification system can be minimized. Toluene was selected to be the VOC source in this study and it is commonly found in semiconductor clean rooms or in painting environments. The odour thresholds of toluene in the range of 1.5–3 ppm were selected for the experiments [42]. This range of toluene concentration could not easily be recognized by human and increases the risk for long period occupational exposure to occupants causing serious health effects to the central nervous system [42].

2. Experimental

2.1. Methodology

An air filtration testing facility was utilized to provide a simulated ventilation ductwork environment for the experiments. The testing system was composed of three sections, i.e. the inlet, the test and the exhaust sections. The schematic diagram of the air filtration testing facility was shown in Fig. 1. The internal walls of the three sections were constructed with glass and stainless steel. The inlet section consisted of a mixing chamber and a converging duct reducing the cross-section area from 0.45 m × 0.45 m (*WH*) to 0.2 m × 0.2 m (*WH*) within a length of 1 m. The air to the mixing chamber was first filtered by a zeolite filter to minimize the influence of background pollution on the testing environment. To generate various relative humidity (RH) levels in the testing system, two refrigeration-type dehumidifiers were installed to reduce the inlet RH level in the inlet air stream. The RH level could be controlled down to 35% with a stability of ±3% at an ambient level of 90% with volume flow rate of 50.4 m^3/h. The RH level could also be controlled up to 95% with a stability of ±3% by two ultra-sonic type humidifiers. Six air heaters with 1000 W each were installed at the air outlet of the dehumidifiers. The inlet air temperature could be controlled in the range of 22–75 °C with a stability of ±1 °C. All the treated air was ducted through the heaters before entering the mixing chamber. Toluene was used as a VOC source in the experiments. The gas phase toluene was generated by bubbling air through a glass bottle containing liquid toluene with purity of 99.5% (BDH Laboratory Supplies). The toluene gas was driven by compressed air and injected to the mixing chamber through a stainless steel pipe. The treated air and toluene were mixed in the mixing chamber and passed through a honeycomb before entering the converging duct. The ozone was injected to the mixed air at the end of the converging duct. This injection location could provide sufficient time for the mixing between the treated air and ozone. It could also minimize the deposition of ozone to the internal wall of the testing system. Ozone was generated by corona discharge principle from two ozone generators (Telewin, Model: Q(FCL)GF005-92) with fan mixers. A 50 L stainless steel reservoir was used and treated as a concentration stabiliser.

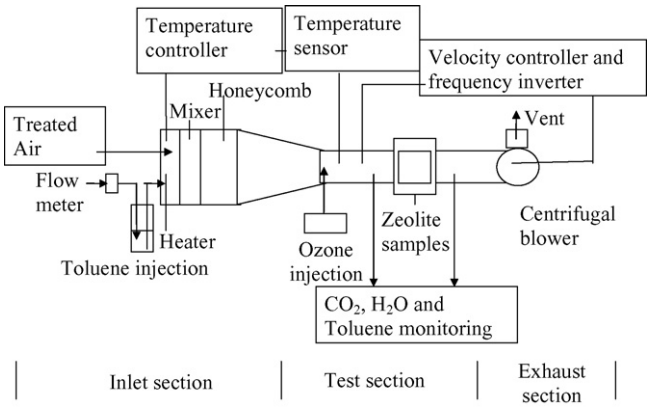

Fig. 1. The schematic diagram of the air filtration system.

The concentration of ozone at the test section was controlled by the ozone generation rate and the volume flow rate between the reservoir and the test section. The ozone concentration could be adjusted ranging from 0 to 6.5 ppm with a stability of ±0.1 ppm. Removable zeolite filters were installed in the test section. The dimension of each of the filter was 30 mm × 200 mm × 200 mm (*LWH*) and a maximum of three filters could be installed for the experiments put in series. The test section was equipped with two sets of sampling ports located 175 mm at the upstream and downstream positions from the filters symmetrically. The outlet of the test section was coupled with the exhaust section. Blower with frequency inverter was installed in the exhaust section so that the air flow rate could be varied in the range of 10–200 m^3/h in the test section with a stability of ±3 m^3/h. The exhaust section was connected to the central exhaust system of the laboratory.

2.2. Instrumentations and procedures

Real-time toluene concentration was measured by a photoacoustic multi-gas monitor (Innova, Model: 1312). The measurement principle is based on the photoacoustic infrared detection method with toluene detection limit of 40 ppb and sample integration time of 5 s. The internal water vapour compensation algorithm in the gas monitor was enabled to minimize the cross-interference between water vapour and toluene. The monitor was calibrated with standard toluene gas in the range of 50–3000 ppb at 40% RH levels. Linear plots of known toluene concentration against the signal strength obtained from the gas monitor were used as the calibration curves. The ozone concentration was monitored by an ozone monitor (API Ozone monitor, Model: 450) based on absorption of 245 nm UV light due to an internal electronic resonance of the ozone molecule. The flow velocity was monitored by a thermo sensor (TSI VelociCalc® Plus, Model: 8386) based on the principle of constant temperature thermal anemometers with a resolution of 0.015 m/s and response time of 200 ms. The RH level was monitored by a thin film capacitive sensor (TSI Q-Trak®, Model: 8551) with a resolution of 0.1% and response time of 20 s. In addition, the CO_2 level was monitored based on the non-dispersive infrared (NDIR) sensor by the same instrument. The temperature in the test section was controlled and monitored by a temperature controller (Cole Parmer Digi Sense, Model: 89000-05) and two K-type thermocouples installed in the test section. The RH, CO_2, toluene and O_3 level were monitored both at the upstream and downstream positions of the zeolite filter.

The zeolite was identified by powdered X-ray diffraction (PXRD) (Philips, Model: PW1830) and also by energy dispersive analysis using X-ray spectrometry (EDAX) (JEOL, Model: JSM 6300). The databases in the joint committee on powder diffraction standards (JCPDS) were used to verify the crystal structure and the phase purity. The bulk chemical composition of the zeolite was measured by the X-ray fluorescence spectroscopy (XRF) (JEOL, Model: JSX-3210Z) element analyser. It is an energy dispersive X-ray fluorescence spectrometer and non-destructive simultaneous quantitative and qualitative analyses of specimens of any shape and size are allowed. Pore surface area of zeolite was determined by using a Brunauer–Emmett–Teller

(BET) surface area analyser (Coulter, Model: SA3100) and nitrogen was used as an adsorbate. The surface area of the samples was determined by physical adsorption of nitrogen at −196 °C. The samples were outgassed at 250 °C for 2 h prior to the nitrogen adsorption–desorption experiments. Specific surface area was calculated from BET-isotherm. The FT-IR spectra, identifying structural features and the adsorption sites at various zeolite 13X samples, were recorded by FT-IR spectroscopy (Bio-Rad, Model: FTS 6000). KBr pellet technique was employed with resolution of 4 cm^{-1}. About 100 mg of dry KBr was mixed with a 10 mg of zeolite and thoroughly mixed by grinding for homogenization. The fine powder was then pressed into a transparent, thin pellet at 5 tonnes cm^{-2}. These thin pellets were used for the normal IR spectral measurements. In addition to the normal IR spectral measurements, the pyridine adsorption method was used for the identification of the specific acid sites in zeolite. The thin pellets was dried at 300 °C for 2 h and cooled to room temperature and a background spectrum was obtained. The thin pellet was allowed to adsorb pyridine in a small stainless steel chamber for 8 min and the excessive pyridine was removed by heating the thin pellets to 100 °C for 30 min. The inferred spectrum in the range of 1400–1700 cm^{-1} was obtained at room temperature for the identification of the adsorbed pyridine at the specific acid sites on the zeolite samples. Air samples for the analysis of VOCs and aldehydes were collected upstream and downstream of the zeolite filter. The downstream air samples were extracted on sorbent tubes (SKC, Model: 226-346) by air sampler (SKC Airchek Sampler, Model: 224-PCXR8) at a flow rate of 200 mL/min in 40 min for Gas Chromatography (Agilent, Model: 6890) and Mass Spectrometry (Agilent, Model: 5973N) analysis following U.S. EPA Method TO-17 for VOC analysis including toluene, 2- and 3-hydroxylated toluene and 2-, and 4-nitrated toluene. The air samples for aldehydes analysis including acetaldehyde, benzaldehyde, formaldehyde and acetone were also extracted on sorbent tubes (SKC, Model: 226-119) by the same sampler at the flow rate of 500 mL/min in 1 h for HP-LC (Hewlett Packard, Model: 1100) analysis following U.S. EPA Method TO-11A.

2.3. Measurement scheme

The zeolite samples were pretreated at 300 °C in an oven for 2 h to remove the organic contaminants and moisture prior to the experiments. Fixed amount of 3600 g zeolite was used with 90 mm zeolite bed-length. Experiments were conducted using 40% RH level. Four different ozone concentrations (0, 1, 4 and 6 ppm) were used and toluene concentrations were maintained also at four different levels (0, 1.5, 2 and 3 ppm). Temperatures were regulated in the experiments. The temperature range in the system was set in the range of 23–25 °C. The inlet CO_2 level was about 700 ppm. The flow velocity was kept constant at 0.35 m/s and thus the residence time for the 90 mm zeolite bed-length was about 0.26 s. The data were recorded at 1 min interval. Each set of experiments was repeated three times and the results were averaged. The conversion C (%) of toluene or ozone was calculated by $C = (C_i - C_o) \times 100/C_i$, where C_i is the inlet concentration and C_o is the outlet concentration at steady state. In order to obtain the amount of adsorbed H_2O and CO_2 in the saturated sample (after adsorption equilibrium), part of the saturated sample (10 g) was extracted to carry out the thermo desorption experiments to quantify the adsorbed H_2O and CO_2 in the samples. The samples were heated at 300 °C in a 5 mm inner diameter quartz tube with the flow of nitrogen at 3 L/min. The outlet of the quartz tube was connected to the photoacoustic multi-gas monitor for the measurement of H_2O and CO_2. The amount of adsorbed species was calculated based on the time for the whole desorption process, mass concentration of each species and the flow rate of the gases at the exit.

3. Results and discussion

The adsorbent was identified as zeolite 13X by PXRD analysis using the JCPDS database (Card no. 39-0218) and it was matched with the chemical formula of $Na_{86}(Al_{86}Si_{106}O_{384})\cdot 264H_2O$. In order to find out the chemical composition of the zeolite sample used in this study, XRF analysis was conducted. The weight percentages of Na, Al and Si element of the zeolite were 12.8%, 25.7% and 53.5%, respectively. The BET surface area of the 13X was found to be 530 m^2/g. The crystal structure of 13X was not damaged by the 6 ppm ozone after three regeneration cycles. The loss of ozone to the wall between the upstream and downstream sampling ports was around 4–7%. It was also observed that around 2–4% of the initial toluene was lost to the wall. The data presented in the following sections have included these background losses of ozone and toluene.

In the tests without the use of zeolite, the conversion of toluene by 6 ppm ozone was about 8% as shown in Fig. 2. The toluene concentration was reduced from 1.5 ppm to about 1.3 ppm. The poor effect of using ozone alone may be due to the fact that the residence time was not enough for ozone to react with the toluene. The residence time for ozone to react with toluene in the system was too short and it was not comparable to the time scale of the ozone–VOC reaction. Weschler [27] stated that the presence of ozone can only alter the concentrations of those specific compounds if the reaction with ozone can occur on a time scale comparable to or faster than the air exchange rate in the building and obviously the time scale in the experimental system was not comparable to the ozone–VOC reaction without zeolite.

3.1. Effect of inlet ozone concentration

The effect of inlet ozone concentration (0–6 ppm) on toluene conversion with zeolite was shown in Fig. 2. The results corresponded to a fixed toluene inlet supply concentration of 1.5 ppm, relative humidity of 40% and 90 mm zeolite bed-length. It was found that the outlet concentration of toluene in all cases dropped to steady states within 3 min. However, the removal performances were different among different ozone concentrations. It was observed that the toluene removal performance was enhanced by ozone. In the case of 0 ppm ozone (i.e. zeolite only), the downstream toluene level was reduced to about

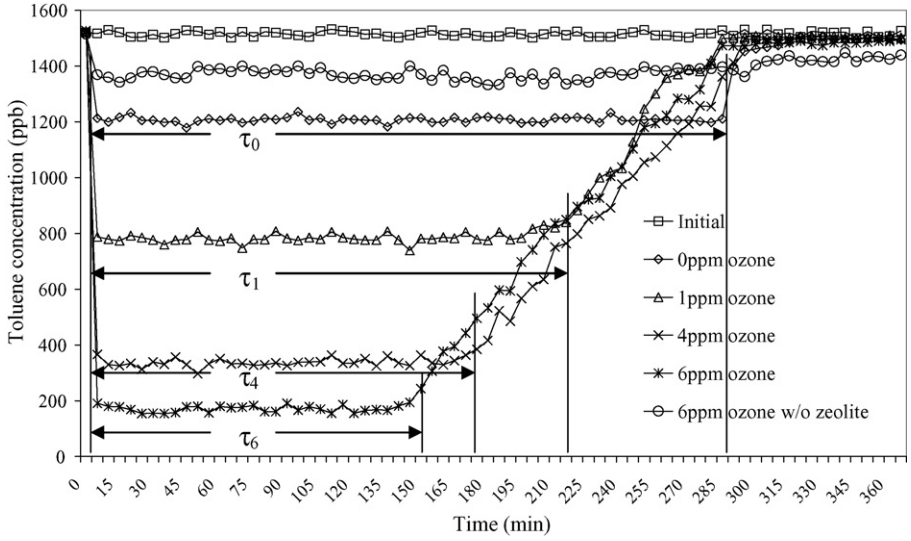

Fig. 2. Effect of ozone inlet concentration on toluene outlet concentration. Experimental conditions: toluene 1.5 ppm, flow rate 50.4 m^3/h, RH 40%, zeolite bed-length 90 mm.

1.2 ppm. Adsorption of toluene to zeolite was the main mechanism for the removal of toluene in this case. With the introduction of various levels of ozone to the system, the removal performance of toluene was enhanced. The toluene level was less than 180 ppb at the downstream position when 6 ppm ozone was used. The conversion of toluene was about 90% in this case. The steady state period τ was defined as the period of time that started at 3 min after running the experiment and stopped when the conversion of toluene started to drop by 10% compared to the steady state condition. From Fig. 2, it was seen that τ was shortened at higher ozone concentrations. In the case of 0 ozone concentration, τ_0 was about 290 min and τ_6 decreased dramatically to about 150 min (nearly half of τ_0) with the increase of the ozone supply concentration to 6 ppm. A possible reason was that during high ozone supply rate, more ozone molecules were attached to the active sites of the zeolite. Toluene decomposition in the active sites of the zeolite could take place more effectively. However, more reaction products together with ozone molecules may occupy the active sites of the zeolite so that τ_6 was much shorter than τ_0. Although the steady state period τ_6 was much shorter than τ_0, the total amount of toluene converted was increased from 371 to 670 mg in the case of 0 and 6 ppm ozone, respectively, during the steady state period.

The consumptions of ozone inside the zeolite structure at different toluene concentrations were summarized in Fig. 3. From Fig. 3, it could be seen that ozone levels diminished significantly after the zeolite filter. In the case of 6 ppm ozone, the ozone outlet concentration was reduced to about 1.2 ppm with over 80% of the ozone consumed. The consumption of ozone was even higher with the presence of 1.5 ppm toluene and the downstream ozone level was reduced by about 90% when 1.5 ppm toluene and 6 ppm ozone were used. This indicated that the zeolite could confine ozone and increase the residence time for reaction between ozone and toluene. The consumption of ozone by zeolite was probably due to the adsorption and the acidic catalytic properties of zeolite 13X.

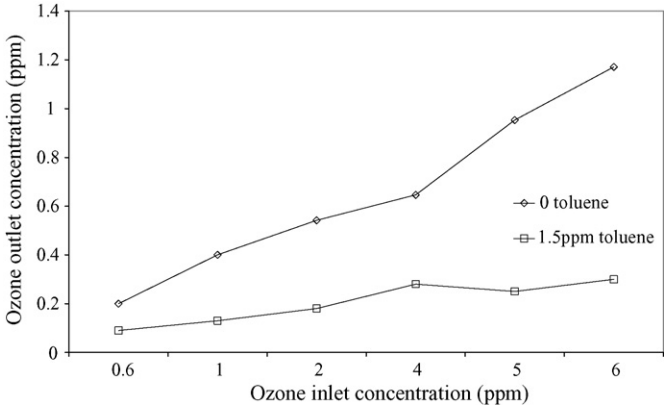

Fig. 3. Effect of toluene inlet concentration on ozone outlet concentration. Experimental conditions: flow rate 50.4 m^3/h, RH 40%, zeolite bed-length 90 mm.

Fig. 4 shows the FT-IR spectrum (1400–1700 cm^{-1}) of the pyridine adsorbed zeolite 13X. Several peaks for the assignments of the adsorbed pyridine at different acid sites were observed. The peaks at 1545 and 1454 cm^{-1} at the FT-IR spectrum were assigned for the Brønsted and the Lewis coordinated

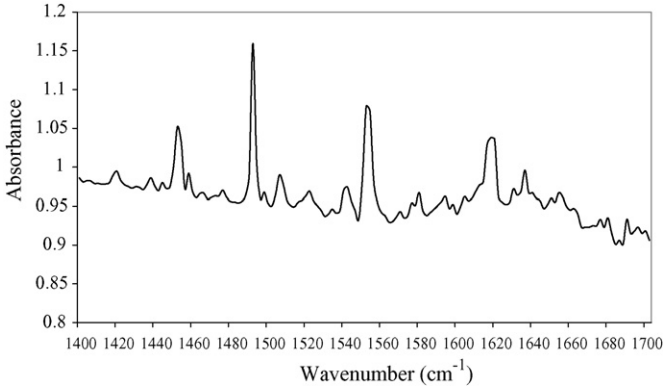

Fig. 4. FT-IR spectrum of pyridine adsorbed on the zeolite.

pyridine, respectively [43]. In addition, the peaks at 1490 and 1620 cm^{-1} represented the adsorption of pyridine at both Brønsted and Lewis acid sites [44]. The FT-IR results confirmed the existence of the acid sites in zeolite 13X. Several studies also showed that the zeolite 13X contains Lewis acid sites. Díaz et al. [45] demonstrated that the total acidity of zeolite 13X was higher than that of H-ZSM-5 and ZSM-5. However, the relative acid strength of zeolite 13X was lower than that of zeolite H-ZSM-5 and ZSM-5. Furthermore, they concluded that the higher selectivity of benzene adsorption than hexane in zeolite 13X was caused by the higher affinity of benzene (Lewis base) with the acid sites. Studies have shown that the decomposition of ozone molecules was based on the existence of Lewis acid sites where significant amount of active oxygen atoms were generated in acid catalyst such as alumina [46,48]. The proposed decomposition mechanism of ozone in these studies was based on the findings on the ozone decomposition mechanisms in MgO [47,49]. The simplified decomposition reactions were expressed with the following sequence of reactions [46,48,49]:

$$O_3 + s \rightarrow sO_3 \quad (1)$$

$$sO_3 \rightarrow sO + O_2 \quad (2)$$

$$sO + O_3 \rightarrow sO_2 + O_2 \quad (3)$$

$$sO_2 \rightarrow s + O_2 \quad (4)$$

"s" in the sequence of reactions represented a surface site, sO_3 was an adsorbed ozone molecule and sO and sO_2 were the surface oxide species. In the current study, we also adopted the proposed decomposition mechanism of ozone in zeolite 13X because of the existence of Lewis acid sites in zeolite 13X which was supported by the FT-IR experiments.

Fig. 5 shows the FT-IR spectrum of the zeolite 13X treated by 6 ppm ozone in the wavenumber range of 1350–1550 cm^{-1}. This range of FT-IR spectrum showed the major difference between the ozone treated zeolite and the blank (desorbed) zeolite. A peak was observed at around 1380 cm^{-1} and it was not observable at the blank zeolites. The peak at 1380 cm^{-1} could attribute to a stable surface oxide species due to a strong M=O bond where the atomic oxygen was attached to a Lewis acid site [46,48,50] on the zeolite surface. This surface oxide species was taken to represent the oxidation product resulting from the ozone treatment on the active surface sites [46]. A similar FT-IR spectrum was also found by Roscoe and Abbatt [46] on the ozone treated alumina surface. From Eq. (2), atomic oxygen was expected to be one of the reaction products of the decomposition of ozone on zeolite. The surface sites "s" could be regenerated through further reaction of sO with ozone via Eqs. (3) and (4) [46,48] provided that sufficient amount of ozone was available to sustain the regeneration process.

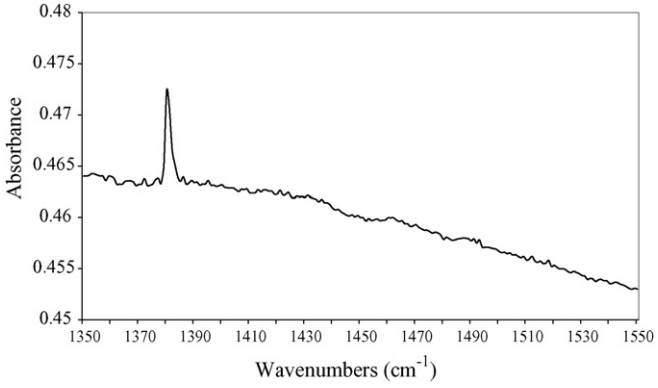

Fig. 5. FT-IR spectrum of ozone adsorbed on the zeolite.

With the presence of toluene, the atomic oxygen from Eq. (2) may undergo the following reaction with toluene:

$$C_6H_5CH_3 + 18O \rightarrow 7CO_2 + 4H_2O \quad (5)$$

The atomic oxygen would attack the C–C and C–H bonds of VOCs and decompose VOCs into CO_2 and H_2O [18]. From Fig. 3, it was observed that when 1.5 ppm toluene was injected to the system, the consumption percentage of 0.6 ppm ozone was increased from 67% to 85%, while it was increased from 80% to 95% at 6 ppm ozone. The increase in ozone consumption implied that extra ozone was used for the decomposition of toluene. When toluene was introduced to the system, the atomic oxygen (O) from Eq. (2) may either go through the regeneration process of the active sites "s" through Eqs. (3) and (4) if sufficient amount of un-reacted ozone was available, or the atomic oxygen would proceed to Eq. (5) for the decomposition of toluene if sufficient amount of atomic oxygen was available. The experimental results showed that saturation occurred after hours of operation as shown in Fig. 2. Ideally, the active sites would be regenerated and atomic oxygen could be produced continuously for the decomposition of toluene. The saturation may be due to the fact that reaction products such as H_2O and CO_2 are generated continuously and some of them occupy the active sites of zeolite. They compete against ozone and toluene adsorption to the active sites so that continuous removal of toluene cannot be sustained. Desorption experiments were conducted to examine the amount of H_2O and CO_2 adsorbed in the deactivated zeolite samples that was treated with 1.5 ppm toluene and 6 ppm ozone. It was assumed that the adsorption/conversion performance of H_2O and CO_2 were uniform in each zeolite pellet. Based on the desorption experiment, it was deduced that 370 g of H_2O and 90 g of CO_2 were adsorbed in the deactivated zeolite (3600 g). The amount of H_2O adsorbed in the deactivated zeolite was about 10% of the total mass of the tested zeolite (3600 g) in which it was very close to the maximum H_2O adsorption capacity of the tested zeolite (about 15% of the total mass). This confirmed that the deactivation of the zeolite was due to the adsorption of H_2O and CO_2 in zeolite. Moreover, the peak representing atomic oxygen attached to Lewis acid site was not observable in the FT-IR spectra of the saturated zeolite sample which confirmed the deactivation of Lewis acid sites for the destruction of ozone. Some studies [51–53] previously stated that H_2O may convert the Lewis sites to Brønsted sites. However, recent study [54] showed the primary effect of H_2O on the acid sites was that H_2O displaced the adsorbed molecules from Brønsted sites and Lewis sites rather than the conversion of Lewis sites to Brønsted sites. The acid sites were occupied by H_2O and hence reduced the decomposition of ozone on the acid

sites. This could further explain the deactivation of the zeolite after a few hours of operations.

3.2. Effect of inlet toluene concentration

Fig. 6 summarizes the influence of various inlet toluene concentrations (1.5, 2 and 3 ppm) on toluene conversion at different ozone concentrations. Results showed that under all inlet toluene concentrations, the toluene conversion increased with the inlet ozone concentration. This was because more ozone was decomposed into atomic oxygen to react with toluene as described in the previous section. However, the results from Fig. 6 indicated that the conversion rate of toluene decreased with the inlet toluene concentration. In the case of 6 ppm ozone, the toluene conversion was about 90% at 1.5 ppm toluene concentration and reduced to about 60% when 3 ppm toluene was maintained at the upstream position. The reduction in conversion percentage may be due to the fact that the amount of ozone was not sufficient to meet the demand of toluene conversion. From Eqs. (1), (2) and (5), the stoichiometric ratio of toluene to ozone was 1:18 for full conversion while the molar ratio of 1.5 and 3 ppm toluene to 6 ppm ozone were about 1:4 and 1:2, respectively. The increase of toluene concentration was moving the toluene to ozone ratio further away from the stoichiometric ratio and hence a reduction in toluene conversion percentage was observed. Fig. 7 shows the ozone conversion corresponding to the experimental conditions in Fig. 6 except the zero ozone condition. It was observed that the ozone conversion increased with the supply concentration of ozone at all the three different toluene concentrations. Since toluene conversion was enhanced by the increase of ozone (as shown in Fig. 6) and thus the consumption of ozone increased with the ozone inlet concentration in Fig. 7. At the instance of 6 ppm ozone inlet concentration, the ozone conversions were above 95% at the three different toluene inlet concentrations. In the cases of 2 and 3 ppm toluene, the conversions of ozone were close to 97%. This indicated that nearly all the supply ozone was consumed. The data indicate that the conversion of toluene is restricted by the inlet concentration of ozone to the system under these specific toluene concentrations.

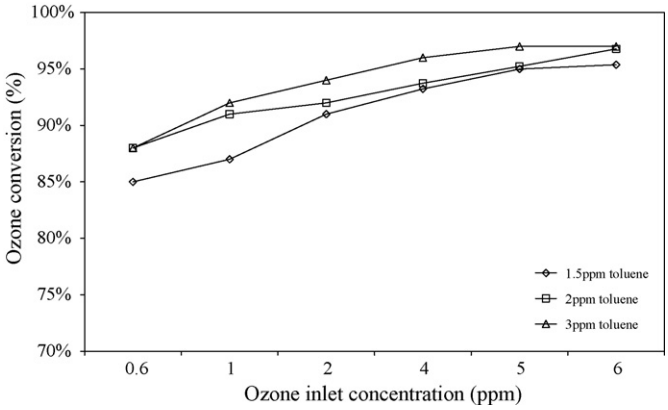

Fig. 7. Effect of ozone inlet concentrations on the conversion of ozone at various toluene inlet concentrations. Experimental conditions: flow rate 50.4 m^3/h, RH 40%, zeolite bed-length 90 mm.

3.3. Products of toluene decomposition

H_2O and CO_2 were believed to be the products of toluene decomposition from Eq. (5). Fig. 8 shows the change of CO_2 and RH levels at 6 ppm ozone at various toluene concentrations. The upstream CO_2 level was about 700 ppm and RH level was set to 40%. It was observed that the CO_2 and RH levels increased with the toluene inlet concentration. When the toluene was not injected to the system (0 ppm toluene), the CO_2 and RH levels were reduced to 337 ppm and 27%, respectively. The reduction was mainly due to the adsorption of H_2O and CO_2 by the zeolite. When 3 ppm toluene was introduced to the system, the CO_2 and RH levels increased to 368 ppm and 34%, respectively. The increases may be due to the reaction products of atomic oxygen and toluene from Eq. (5) or because of the fact that some of the active sites of the zeolite were occupied by toluene reducing the adsorption of CO_2 and H_2O.

In addition to CO_2 and H_2O, downstream gaseous samples were extracted to sorbent tubes for HP-LC and GC–MS analysis. Table 1 showed the results of the GC–MS and HP-LC analysis with two different ozone levels (1 and 6 ppm) at 1.5 ppm toluene inlet concentration. From the results of GC–MS analysis, the hydroxylated and nitrated toluenes were not detected

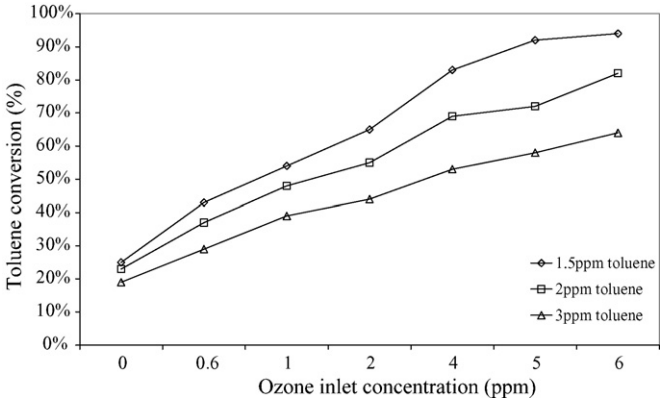

Fig. 6. Effect of toluene inlet concentrations on the conversion of toluene at various ozone inlet concentrations. Experimental conditions: flow rate 50.4 m^3/h, RH 40%, zeolite bed-length 90 mm.

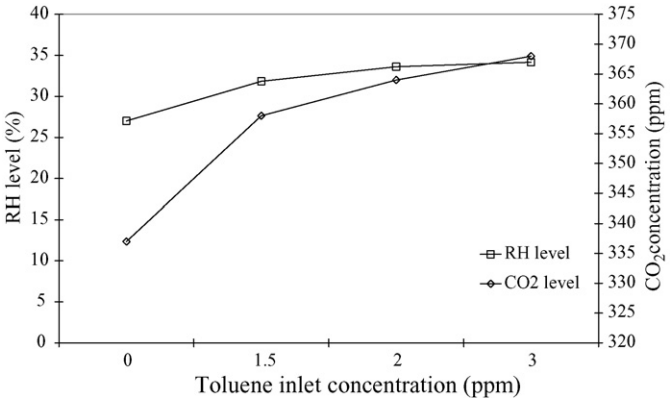

Fig. 8. Effect of toluene inlet concentration on downstream RH and CO_2 levels. Experimental conditions: flow rate 50.4 m^3/h, RH 40%, ozone 6 ppm, CO_2 700 ppm, zeolite bed-length 90 mm.

Table 1
Steady state concentration of the by-products at downstream position with 1 ppm and 6 ppm ozone

Species	Analytical methods	Species concentration (ppb)	
Upstream ozone	UV absorption	1000	6000
Toluene	GC–MS	780	192
2-Hydroxylated toluene	GC–MS	Not detected	Not detected
3-Hydroxylated toluene	GC–MS	Not detected	Not detected
2-Nitrated toluene	GC–MS	Not detected	Not detected
4-Nitrated toluene	GC–MS	Not detected	Not detected
Acetaldehyde	HP-LC	<10	46
Acetone	HP-LC	Not detected	Not detected
Benzaldehyde	HP-LC	Not detected	38
Formaldehyde	HP-LC	<10	44

Experimental conditions: toluene 1.5 ppm, flow rate 50.4 m^3/h, RH 40%, zeolite bed-length 90 mm.

in the downstream gaseous samples in both cases. This implied the reactive hydroxylated and nitrated species were not generated by the ozone–toluene reaction, or even if generated, they were held effectively by the zeolite. However, these species were found in the decomposition of toluene with a surface discharge microplasma device using similar decomposition mechanisms [18]. Trace amount (<50 ppb) of acetaldehyde, benzaldehyde and formaldehyde were found to be the intermediate species when 6 ppm ozone was used. These may be due to the partial oxidation of toluene by atomic oxygen. No other significant by-products were identified by the sampling and the analytical methods employed in this study. The intermediate species could be minimized by increasing the bed-length of the zeolite reactor so that they could be adsorbed or reacted subsequently.

4. Conclusions

The decomposition of gas phase toluene by ozone in zeolite 13X was studied in an air filtration testing facility. The toluene decomposition efficiency was affected by the inlet concentration of ozone. The steady state period for the treatment of 1.5 ppm toluene was reduced from 290 to 150 min when 0 and 6 ppm ozone was used, respectively. This reduction could be due to the fact that the reaction sites of the zeolite were occupied by ozone, H_2O, CO_2 and reaction by-products which caused the deactivation of the zeolite in a few hours. The removal percentage of 1.5 ppm toluene by the adsorption of zeolite was about 25% without the presence of ozone while over 90% of toluene was removed with the use of 6 ppm ozone. This was probably because the atomic oxygen was generated during the decomposition of ozone on the Lewis acid sites in the zeolite. FT-IR results indicated that the zeolite treated by 6 ppm ozone showed a distinctive peak at 1380 cm^{-1} in which it was attributed to surface oxide species. The atomic oxygen was attached to a Lewis acid site in the zeolite. The toluene conversion was also influenced by the inlet toluene concentration. The reduction in the conversion percentage with the increase of toluene inlet concentration may be due to the fact that the amount of ozone was not sufficient to meet the demand of the conversion. The stoichiometric ratio of toluene to ozone was 1:18 and this ratio was crucial for the effectiveness of toluene to be removed by zeolite and ozone. The CO_2 and RH levels were found to increase when toluene was injected to the system with the presence of ozone. The increase may be due to the reaction products of toluene–ozone reaction or because some of the active sites of zeolite were occupied by toluene. HP-LC analysis showed that trace amounts (<50 ppb) of acetaldehyde, benzaldehyde and formaldehyde were found in the downstream gaseous samples when 1.5 ppm toluene and 6 ppm ozone were used. This may be due to the partial oxidation products of toluene by atomic oxygen.

The experimental results suggest that the toluene to ozone ratio is crucial for the elimination of toluene. More experiments need to be conducted to investigate the proper toluene to ozone ratio in order to obtain the best toluene elimination performance with minimum residue ozone level. In addition, more zeolite can be used to minimize the amount of the generated by-products. Saturation occurs after hours of operation and this may be due to the adsorption of CO_2 and H_2O onto the active sites of zeolite. Experiments on thermo desorption of the deactivated zeolite showed that the adsorption of H_2O was around 10% of the total mass of the tested samples and this could deactivate the conversion of toluene. Based on the experimental results, selection of other kinds of zeolite avoiding the adsorption of water so that more active sites can be released for the VOCs and ozone will be a method to enhance the VOC destruction rate and also the saturation level so as to void too frequent regeneration need. This study demonstrated the potential use of a coupled ozone and zeolite system in removing VOCs such as toluene.

Acknowledgements

The authors would like to thank the technical supports from Materials Characterization and Preparation Facilities (MCPF) and Advanced Engineering Materials Facility (AEMF) at the Hong Kong University of Science and Technology for the PXRD, FT-IR and BET analysis. Funding for this research was provided by RGC Grant HKUST 6132/04E.

References

[1] U.S. Environmental Protection Agency (USEPA), Sources of indoor air pollution—organic gases (volatile organic compounds, VOCs). http://www.epa.gov/iaq/voc.html.

[2] P. Hunter, S.T. Oyama, Control of Volatile Organic Compound Emissions, Conventional and Emerging Technologies, Wiley-Interscience, New York, 2000.
[3] S.K. Kjaergaard, L. Molhave, Human reactions to a mixture of indoor air volatile organic compounds, Atmos. Environ. A 25 (8) (1991) 1417–1426.
[4] H.S. Brightman, N. Moss, Sick Building Syndrome Studies and the Compilation of Normative and Comparative Values, Indoor Air Quality Handbook, McGraw-Hill, New York, 2001.
[5] S. Uchiyama, S. Hasegawa, Investigation of a long-term sampling period for monitoring volatile organic compounds in ambient air, Environ. Sci. Technol. 34 (2000) 4656–4661.
[6] S. Brosillon, M.H. Manero, J.N. Foussard, Mass transfer in VOC adsorption on zeolite: experimental and theoretical breakthrough curves, Environ. Sci. Technol. 35 (2001) 3571–3575.
[7] M.V. Chandak, Y.S. Lin, Hydrophobic zeolites as adsorbents for removal of volatile organic compounds from air, Environ. Technol. 19 (1998) 941–948.
[8] F. Delage, P. Pre, P.L. Cloirec, Mass transfer and warming during adsorption of high concentrations of VOCs on an activated carbon bed: experimental and theoretical analysis, Environ. Sci. Technol. 34 (2000) 4816–4821.
[9] X.S. Zhao, Q. Ma, G.Q.M. Lu, VOC Removal: comparison of MCM-41 with hydrophoblic zeolites and activated carbon, Energy Fuel 12 (1998) 1051–1054.
[10] K. Everaert, J. Baeyens, Catalytic combustion of volatile organic compounds, J. Hazard. Mater. 109 (1–3) (2004) 113–139.
[11] A. O'Reilly, A series reaction approach to VOC incineration, Process Saf. Environ. 76 (B4) (1998) 302–312.
[12] M.A. Alvarez-Merino, M.F. Ribeiro, J.M. Silva, F. Carrasco-Mariän, F.J. Maldonado-Hoädar, Activated carbon and tungsten oxide supported on activated carbon catalysts for toluene catalytic combustion, Environ. Sci. Technol. 38 (2004) 4664–4670.
[13] D.T. Tompkins, W.A. Zeltner, B.J. Lawnicki, M.A. Anderson, Evaluation of photocatalysis for gas-phase air cleaning. Part 1. Process, technical and sizing considerations, ASHRAE Trans. 111 (2005) 60–84.
[14] D.T. Tompkins, W.A. Zeltner, B.J. Lawnicki, M.A. Anderson, Evaluation of photocatalysis for gas-phase air cleaning. Part 2. Economics and utilization, ASHRAE Trans. 111 (2005) 85–95.
[15] P. Zhang, F. Liang, G. Yu, Q. Chen, W. Zhu, A comparative study on decomposition of gaseous toluene by O_3/UV, TiO_2/UV and O_3/TiO_2/UV, J. Photochem. Photobiol. A: Chem. 156 (2003) 189–194.
[16] A.T. Hodgson, D.P. Sullivan, W.J. Fisk, Parametric evaluation of an innovative ultra-violet photocatalytic oxidation (UVPCO) air cleaning technology for indoor applications, Report No. LBNL-59074, Lawrence Berkeley National Laboratory, Berkeley, CA, 2005.
[17] S. Oh, H. Kim, A. Ogata, H. Einaga, S. Futamura, D. Park, Effect of zeolite in surface discharge plasma on the decomposition of toluene, Catal. Lett. 99 (1/2) (2005) 101–104.
[18] T. Seto, S.B. Kwon, M. Hirasawa, A. Yabe, Decomposition of toluene with surface-discharge microplasma device, Jpn. J. Appl. Phys. 44 (2005) 5206–5210.
[19] H. Einaga, T. Ibusuki, S. Futamura, Performance evaluation of a hybrid system comprising silent discharge plasma and manganese oxide catalysts for benzene decomposition, IEEE Trans. Ind. Appl. 37 (2001) 1476–1482.
[20] A. Ogata, H. Einaga, H. Kabashima, S. Futamura, S. Kushiyama, H.H. Kim, Effective combination of nonthermal plasma and catalysts for decomposition of benzene in air, Appl. Catal. B: Environ. 46 (2003) 87–95.
[21] U.S. Environmental Protection Agency (USEPA). Ozone generators that are sold as air cleaners: an assessment of effectiveness and health consequences, ozone generator fact sheet. http://www.epa.gov/iaq/pubs/ozonegen.html.
[22] K.P. Yu, G.W.M. Lee, C.P. Hsieh, S.H. Yang, Using ozone air cleaners to remove indoor volatile organic compounds, in: Proceedings of the 10th International Conference on Indoor Air Quality, Indoor Air 2005, Beijing, China, September 4–9, 2005, pp. 2981–2985.
[23] M. Boeniger, Use of ozone generating devices to improve indoor air quality, Am. Ind. Hyg. Assoc. J. 56 (1995) 590–598.
[24] H.F. Hubbard, B.K. Coleman, G. Sarwar, R.L. Corsi, Effects of an ozone-generating air purifier on indoor secondary particles in three residential dwellings, Indoor Air 15 (2005) 432–444.
[25] M. Lippmann, Health effects of ozone: a critical review, J. Air Pollut. Control Assoc. 39 (1989) 672–695.
[26] U.S. Environmental Protection Agency (USEPA), Health and environmental effects of ground-level ozone. OAQPS Fact Sheet, 1997. http://www.epa.gov/ttn/oarpg/naaqsfin/o3health.html.
[27] C.J. Weschler, Ozone in indoor environments: concentration and chemistry, Indoor Air 10 (2000) 269–288.
[28] Z. Fan, P. Lioy, C. Weschler, N. Fiedler, H. Kipen, J. Zhang, Ozone-initiated reactions with mixtures of volatile organic compounds under simulated indoor conditions, Environ. Sci. Technol. 37 (2003) 1811–1821.
[29] H. Destaillats, B.C. Singer, B.K. Coleman, M.M. Lunden, A.T. Hodgson, C.J. Weschler, W.W. Nazaroff, Secondary pollutants from cleaning products and air fresheners in the presence of ozone, in: Proceedings of the 10th International Conference on Indoor Air Quality, Indoor Air 2005, Beijing, China, September 4–9, 2005, pp. 2081–2085.
[30] W. Chen, J.S. Zhang, Z. Zhang, Performance of air cleaners for removing multiple volatile organic compounds in indoor air, ASHRAE Trans. 111 (2005) 1101–1114.
[31] S.T. Oyama, Chemical and catalytic properties of ozone, Catal. Rev. Sci. Eng. 42 (2000) 279–322.
[32] J.R. Kastner, Q. Buquoi, R. Ganagavaram, K.C. Das, Catalytic ozonation of gaseous reduced sulfur compounds using wood fly ash, Environ. Sci. Technol. 39 (2005) 1835–1842.
[33] J.R. Kastner, K.C. Das, N.D. Melear, Catalytic oxidation of gaseous reduced sulfur compounds using coal fly ash, J. Hazard. Mater. 95 (2002) 81–90.
[34] V. Gomez-Serrano, P.M. Alverez, J. Jaramillo, F.J. Beltran, Formation of oxygen structures by ozonation of carbonaceous materials prepared from cherry stones. II. Kinetic study, Carbon 40 (4) (2002) 523–529.
[35] H. Valde's, M. Sa'nchez-Polo, J. Rivera-Utrilla, C. Zaror, Effect of ozone treatment on surface properties of activated carbon, Langmuir 18 (2002) 2111–2116.
[36] J. You, H. Chiang, P. Chiang, Comparison of adsorption characteristics for VOCs on activated carbon and oxidized activated carbon, Environ. Prog. 13 (1) (1994) 31–36.
[37] D.W. Breck, Zeolite Molecular Sieves: Structure Chemistry and Use, Krieger Publishing Company, Malabar, FL, 1984.
[38] B.C. Gates, Catalytic Chemistry, Wiley, New York, 1992.
[39] E.V. Bavel, V. Meynen, P. Cool, E.F. Vansant, Adsorption of hydrocarbons on mesoporous phts materials, Langmuir 21 (2005) 2447–2453.
[40] I. Tsukada, S. Higuchi, Pulsed-laser deposition of $LiNbO_3$ in low gas pressure using pure ozone, Jpn. J. Appl. Phys. 43 (2004) 5307–5312.
[41] W. Song, G. Li, V.H. Grassian, S.C. Larsen, Development of improved materials for environment applications: nanocrystalline NaY zeolites, Environ. Sci. Technol. 39 (2005) 1214–1220.
[42] Occupational Safety and Health Administration (OSHA), US Department of Labor, Occupational Safety and Health Guideline for Toluene, 1996. http://www.osha.gov/SLTC/healthguidelines/toluene/recognition.html.
[43] F. Collignon, G. Poncelet, Comparative vapor phase synthesis of ETBE from ethanol and isobutene over different acid zeolites, J. Catal. 202 (2001) 68–77.
[44] M.R. Basila, T.R. Kantner, K.H. Rhee, The nature of the acidic sites on a silica–alumina. Characterization by infrared spectroscopic studies of trimethylamine and pyridine chemisorption, J. Phys. Chem. 68 (1964) 3197–3207.
[45] E. Díaz, S. Ordónez, A. Vega, J. Coca, Evaluation of different zeolites in their parent and protonated forms for the catalytic combustion of hexane and benzene, Micropor. Mesopor. Mater. 83 (2005) 292–300.
[46] J.M. Roscoe, J.P.D. Abbatt, Diffuse Reflectance FTIR study of the interaction of alumina surfaces with ozone and water vapour, J. Phys. Chem. 109 (2005) 9028–9034.
[47] H. Einaga, S. Futamura, Catalytic oxidation of benzene with ozone over alumina-supported manganese oxides, J. Catal. 227 (2004) 304–312.
[48] R.C. Sullivan, T. Thornberry, J.P.D. Abbatt, Ozone decomposition kinetics on alumina: effects of ozone partial pressure, relative humidity and repeated oxidation cycles, Atmos. Chem. Phys. 4 (2004) 1301–1310.
[49] W. Li, G.V. Gibbs, S.T. Oyama, Mechanism of ozone decomposition on a manganese oxide catalyst. 1. In situ Raman spectroscopy and ab

initio molecular orbital calculations, J. Am. Chem. Soc. 120 (1998) 9041–9046.

[50] K. Thomas, P.E. Hoggan, L. Mariey, J. Lamotte, J.C. Lavalley, Experimental and theoretical study of ozone adsorption on alumina, Catal. Lett. 46 (1997) 77–82.

[51] R.A. Comelli, C.R. Vera, J.M. Parera, Influence of ZrO_2 crystalline structure and sulfate ion concentration on the catalytic activity of $SO_4^{2-}ZrO_2$, J. Catal. 151 (1995) 96–101.

[52] C. Morterra, G. Cerrato, F. Pinna, M. Signoretto, G. Strukul, On the acid-catalyzed isomerization of light paraffins over a ZrO_2/SO_4 system: the effect of hydration, J. Catal. 149 (1994) 181–188.

[53] F. Babou, G. Coudurier, J.C. Vedrine, Acidic properties of sulfated zirconia: an infrared spectroscopic study, J. Catal. 152 (1995) 341–349.

[54] A.P. Kulkarni, A.S. Muggli, The effect of water on the acidity of TiO_2 and sulfated titania, Appl. Catal. A: Gen. 302 (2006) 274–282.